Published in IET Microwaves, Antennas & Propagation
Received on 12th September 2008
Revised on 26th February 2009
doi: 10.1049/iet-map.2008.0315

ISSN 1751-8725

Design of a double-layered spiral antenna for radio frequency identification applications

C. Lee[1] *W.K. Han*[2] *I. Park*[3] *H. Choo*[1]

[1]*School of Electronic and Electrical Engineering, Hongik University, Seoul, Korea*
[2]*Department of Physics, Hongik University, Seoul, Korea*
[3]*School of Electrical and Computer Engineering, Ajou University, Suwon, Korea*
E-mail: hschoo@hongik.ac.kr

Abstract: In this study, the authors describe a novel circularly polarised (CP) double-layered spiral antenna (DLSA) consisting of two main spiral radiators printed on a thin substrate, a feed line and a folded ground plane for a ultra-high-frequency (UHF) band radio frequency identification (RFID) reader. The proposed antenna exhibits broad impedance and CP bandwidth characteristics. The fabricated prototype has an axial ratio of less than 3 dB, a return loss of less than −10 dB over an 860–960 MHz range and a gain of 6.7 dB in the operating frequency range. This performance confirms that the proposed antenna is appropriate for commercial RFID use in the UHF band.

1 Introduction

Radio frequency identification (RFID) in the ultra-high-frequency (UHF) band transfers ID information from a tag to a reader using an RF backscattering mechanism. Most RFID tag antennas radiate a linear polarised electromagnetic wave, and to achieve reception stability that is independent of the tag's polarisation, reader antennas should be designed to maintain circularly polarised (CP) radiation characteristics [1]. The antenna of the reader should also have broad impedance and CP bandwidth of 860–960 MHz to be compatible with all regional frequency standards [2]. The reader antenna should also be small for better portability and ease of installation. Many current RFID reader antennas have a microstrip patch structure with various CP excitation schemes such as truncating the edge of the patch or phase shifting the feed network to obtain a broadband CP characteristic [3–7]. Although such microstrip patches do produce CP radiation, the CP bandwidth and matching bandwidth cannot easily cover the worldwide UHF RFID frequency band simultaneously [8]. Antennas with a spiral structure have been proposed to solve these problems of microstrip patches since the spiral structure inherently provides a broad CP characteristic because of its travelling wave excitation. However, these spiral antennas have the drawbacks of a bigger antenna body and ground plane [9, 10].

In this paper, we propose a double-layered spiral antenna (DLSA) with broad impedance matching and CP characteristics for use as a RFID reader in the UHF band. The double-layered spiral arms produce a broad CP bandwidth with a small antenna size [11]. A quarter-wave transformer is inserted between the spiral antenna body and the coaxial feed to broaden the matching bandwidth by stepping down the high impedance of the spiral antenna arm [12, 13]. In addition, the edge of the ground plate is folded to reduce the size of the ground plane and simultaneously maintain the broad CP characteristic. A prototype of the antenna was fabricated and the measured antenna performance demonstrated that the DLSA is superior to conventional microstrip patch antennas.

2 Antenna structure and results

Fig. 1 shows the geometry of the proposed DLSA, which consists of two-layered spiral arms printed on an FR-4 substrate, a quarter-wave transformer and a folded ground plane. A polygonally wound spiral structure is used to broaden the CP bandwidth as shown in Figs. 1*a* and 1*b*. The bending points are determined by the step angle ($\theta_n = 45^\circ \times n$) and the length ($r_{(n)}$) from the origin to form the spiral structure. Each spiral turn ($NT = 1$) corresponds to an increase in n of 8. Since this polygonally wound

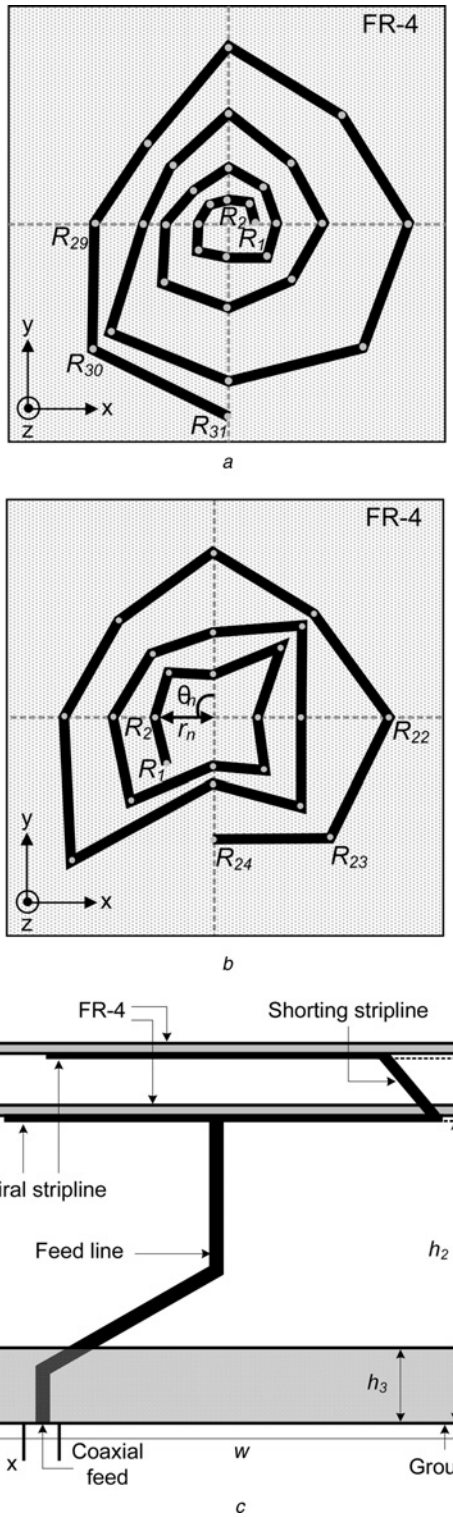

Figure 1 *Geometry and design parameters of the proposed DLSA*

a Top view of the upper layer
b Top view of the lower layer
c Side view

structure has more design flexibility in controlling the induced current of the spiral arm, it can provide current more similar to a travelling wave, which is essential for broad CP operation. Thus, the proposed antenna can have better phase linearity and broader CP bandwidth for a given diameter of the outside spiral radius. The 2-mm-wide stripline ($\sigma = 5.8 \times 10^7$) is printed on a thin FR-4 substrate ($\varepsilon_r = 4.25$, tan $\delta = 0.02$, thickness = 1.6 mm). Two layered spiral arms are used because the bandwidth and CP bandwidth of the double-layered spiral are superior to the single-layer spiral with the same ground plane size and height in our electromagnetic (EM) simulation. The stripline on the lower layer is wound clockwise from the outside towards the centre and the upper stripline is also wound clockwise from the centre outward to produce right-hand CP radiation. The outer endpoints of the two spiral arms are connected by a shorting stripline. The 2-mm-wide stripline ($\sigma = 5.8 \times 10^7$) is printed on a thin FR-4 substrate ($\varepsilon_r = 4.25$, tan $\delta = 0.02$, thickness = 1.6 mm). Fig. 1*c* shows the slightly slanted feed stripline between the coaxial feed and the lower spiral arm that operates similar to a quarter-wave transformer. The slanted feed line can be considered a tapered two-wire transmission line from the image theory. The characteristic impedance of the slanted line increases from about 50 to 200 Ω [14]. This slanted feed line can thus change the high impedance of the CP spiral arm from the impedance close to 50 Ω at the coaxial feed. A ground plane area of greater than about $0.7 \times 0.7\ \lambda$ ($f_c = 912$ MHz) is required to maintain the CP characteristic over a broad bandwidth. The big ground plane increases the overall size of the antenna. To reduce the size of the ground plane, we folded up each edge of the ground plate by 20.6 mm ($h_3 = 0.06\ \lambda$). This folded structure seems to operate as an open-ended cavity to increase the effective ground area [15, 16]. It can, therefore, reduce the size of the ground plane while maintaining the broad CP characteristic.

To obtain the detailed design parameters (r_{mn}, h_1, h_2, h_3, w and NT) and achieve the stated design goals of broad impedance bandwidth, CP bandwidth and small size, we used the Pareto genetic algorithm (PGA) in conjunction with the FEKO EM simulation tool [17–20]. The cost functions of the PGA algorithm to produce the optimised

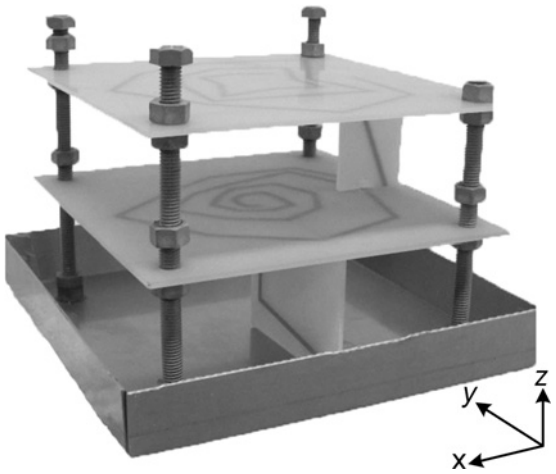

Figure 2 *Prototype antenna*

doi: 10.1049/iet-map.2008.0315

Table 1 Design parameters for the antenna arm

(a) First layer																
wire number		R_1	R_2	R_3	R_4	R_5	R_6	R_7	R_8	R_9	R_{10}	R_{11}	R_{12}	R_{13}	R_{14}	R_{15}	R_{16}
position, mm	x	6.8	5.4	0.0	−4.9	−7.6	−7.9	0.0	9.7	12.4	9.2	0.0	−8.6	−15.8	−16.7	0.0	16.0
	y	0.0	5.4	6.3	4.9	0.0	−7.9	−9.5	−9.7	0.0	9.2	14.9	8.6	0.0	−16.7	−23.4	−16.5
wire number		R_{17}	R_{18}	R_{19}	R_{20}	R_{21}	R_{22}	R_{23}	R_{24}	R_{25}	R_{26}	R_{27}	R_{28}	R_{29}	R_{30}	R_{31}	a
position, mm	x	24.2	16.1	0.0	−14.9	−21.3	−30.0	0.0	34.1	45.7	28.9	0.0	−20.8	−33.8	−34.5	0.0	49.0
	y	0.0	16.1	29.6	14.9	0.0	−30.0	−43.5	−34.1	0.0	28.9	47.9	20.8	0.0	−34.5	−52.7	0.0

(b) Second layer																	
wire number		R_1	R_2	R_3	R_4	R_5	R_6	R_7	R_8	R_9	R_{10}	R_{11}	R_{12}				
position, mm	x	−14.1	−17.5	−13.3	0.0	21.0	13.7	15.8	0.0	−25.0	−30.4	−18.6	0.0				
	y	−14.1	0.0	13.3	12.3	21.0	0.0	−15.8	−14.4	−25.0	0.0	18.6	25.2				
wire number		R_{13}	R_{14}	R_{15}	R_{16}	R_{17}	R_{18}	R_{19}	R_{20}	R_{21}	R_{22}	R_{23}	R_{24}				
position, mm	x	27.2	27.0	27.0	0.0	−43.0	−45.2	−28.7	0.0	30.8	53.9	35.8	0.0				
	y	27.2	0.0	−27.0	−19.8	−43.0	0.0	28.7	30.8	30.8	0.0	−35.8	−36.3				

design parameters are given in (1)–(3)

$$\text{Cost1} = 1 - \frac{\text{BW}_{\text{reader}} \times \text{Eff}_{\text{reader}}}{\text{BW}_{\text{RFID}}} \quad (1)$$

$$\text{Cost2} = 1 - \frac{\text{CPBW}_{\text{reader}}}{\text{BW}_{\text{RFID}}} \quad (2)$$

$$\text{Cost3} = w(\text{antenna size}) \quad (3)$$

Equation (1) is the product of the radiation efficiency ($\text{Eff}_{\text{reader}}$) and the impedance bandwidth ($\text{BW}_{\text{reader}}$) of the test antenna. Equation (2) takes into account the CP bandwidth and (3) is included to reduce the size of the antenna. In our optimisation, a lower cost function means better performance. The Cost1 value of 0 means a 10% bandwidth and the value of 1 indicates a 0% bandwidth. To decrease the EM simulation time required for the optimisation process, the stripline printed on the substrate was modelled as a conducting wire with a radius of 1 mm and a dielectric coating of 2 mm radius [21].

Fig. 2 is a photo of the DLSA fabricated according to the design based on 300 PGA iterations. The optimised antenna has NT = 3.5 for the upper spiral arm and NT = 3 for the lower spiral arm. The heights of the antenna arms (h_1 and h_2) are 4.2 and 8.2 cm, respectively, and the whole length of the antenna stripline including the shorting stripline is about 5.2 λ (f_c 912 MHz). The size of the ground plate (w) and the height of the folded edge (h_3) are 14 and 2 cm, respectively. Table 1 shows the detailed dimensions of the bending points of the optimised spiral arms.

The performance of the fabricated DLSA was characterised and compared with the results of the simulation. Fig. 3 shows the return losses and the axial ratio (AR) of the DLSA. The measured impedance bandwidth ($S_{11} < -10$ dB) was 17% (805–960 MHz) and the CP bandwidth (AR < 3 dB) was 20% (850–1000 MHz), so the antenna can cover the full UHF RFID band (860–960 MHz). Fig. 4 shows the gain of the DLSA. Both the measured and simulated gain approach is about 6.5 dB, which is appropriate for a RFID reader according to the EIRP regulation for an input power of 1 W [22].

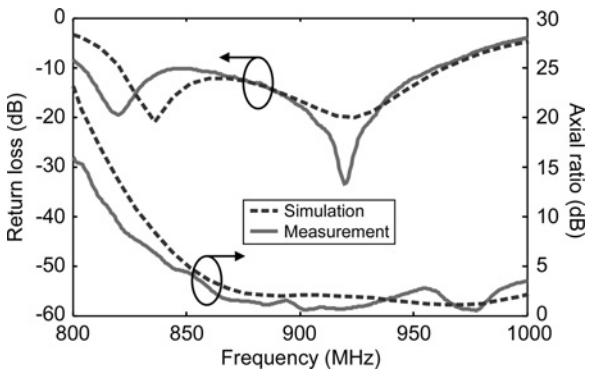

Figure 3 *Measured and simulated return loss and axial ratio of the DLSA*

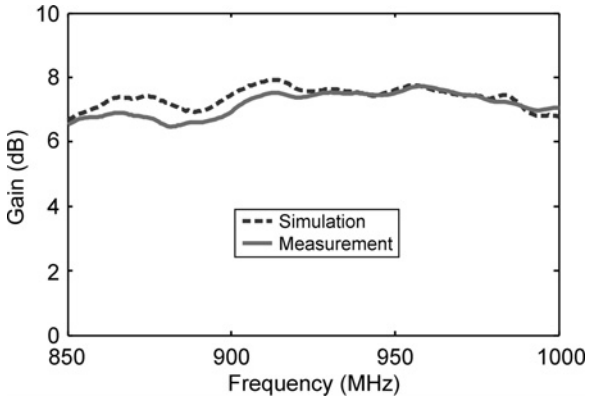

Figure 4 *Measured and simulated gain of the DLSA*

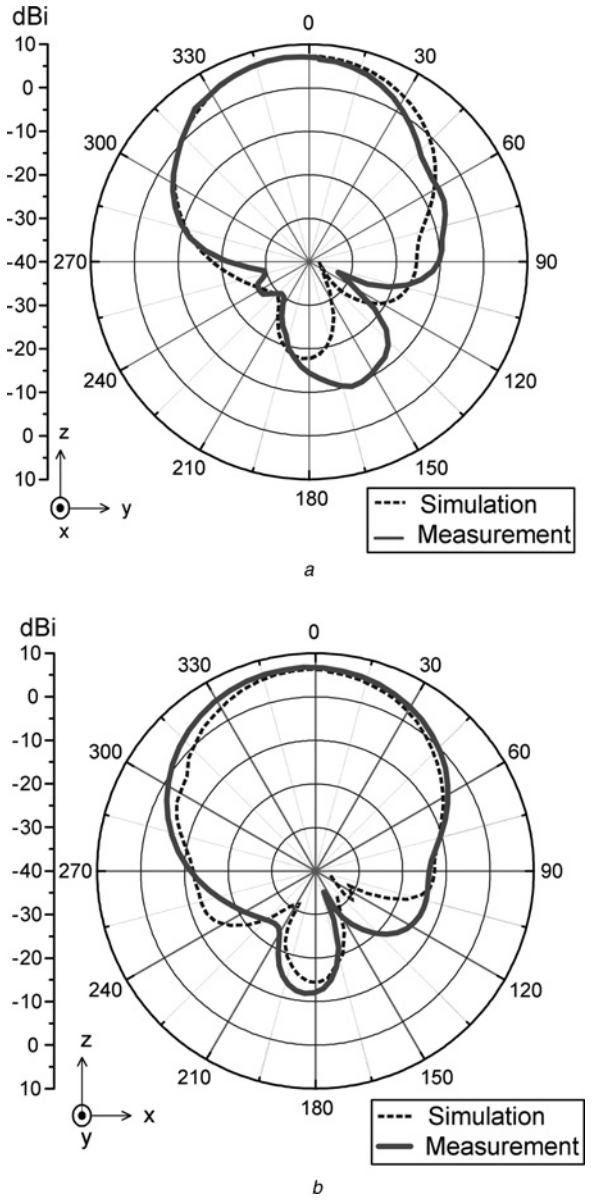

Figure 5 *Measured radiation patterns of the antenna (912 MHz) in the*

a *x–z* plane
b *y–z* plane

doi: 10.1049/iet-map.2008.0315

Figs. 5*a* and 5*b* illustrate the radiation patterns of the antenna at 912 MHz. The antenna exhibited similar beam shapes in the $x-z$ and $y-z$ planes with half-power beamwidths of 87 and 91°, respectively. To measure the reading range of the DLSA, we installed it on a CS-461 RFID reader system [23] and measured the maximum reading distance of the ALL-9440 (Gen2 Squiggle) tag antenna [24]. The solid and dashed lines in Fig. 6 indicate the reading ranges of the DLSA for co- and cross-polarised tag antenna orientations, respectively. The results show a maximum reading range of 3.4 m in the bore-sight direction, and similar reading areas of 9.42 m^2 for the co-polarisation and 9.21 m^2 for the cross-polarisation of the tag.

3 Antenna analysis

A CP antenna should have a current distribution similar to that of a travelling wave to achieve broad CP characteristics [11]. To interpret the broadband CP characteristics of the DLSA, the phase and the amplitude of the induced current on the stripline were analysed using the FEKO EM simulation tool at 912 MHz; the results are shown in Fig. 7. The phase of the current on the stripline decays in a nearly linear fashion, forming a travelling wave on the spiral arm. This travelling wave permits broadband CP operation [25].

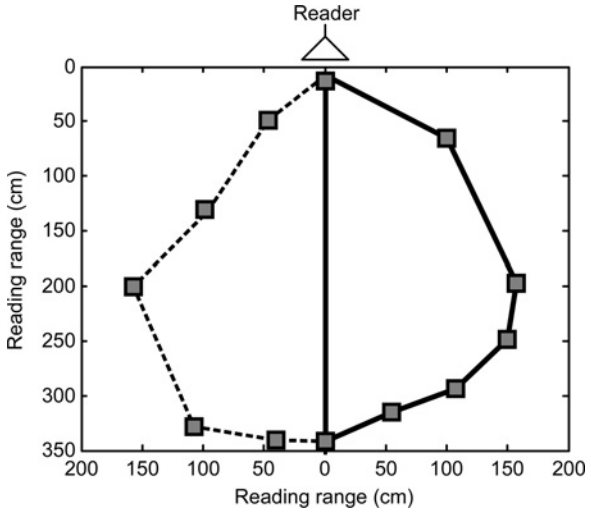

Figure 6 *Reading range of the proposed antenna*

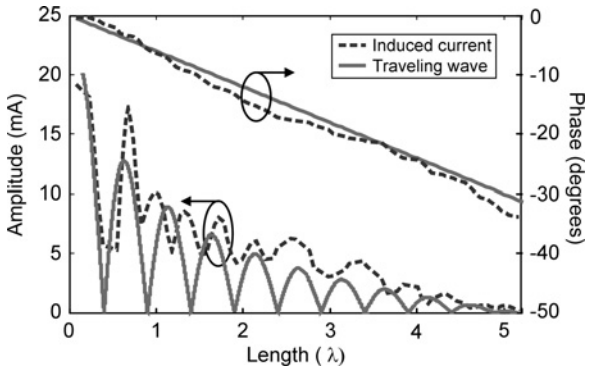

Figure 7 *Amplitude and phase of the induced current at 912 MHz*

We created the equivalent resistor, inductor and capacitor (RLC) circuit model for the proposed antenna to clarify the operating principle of the broad impedance bandwidth. The DLSA arms were modelled using two parallel RLC resonance circuits, and the slanted feed line was modelled as a quarter-wave impedance transformer as shown in Fig. 8*a*. Then each value of the lumped element was obtained using

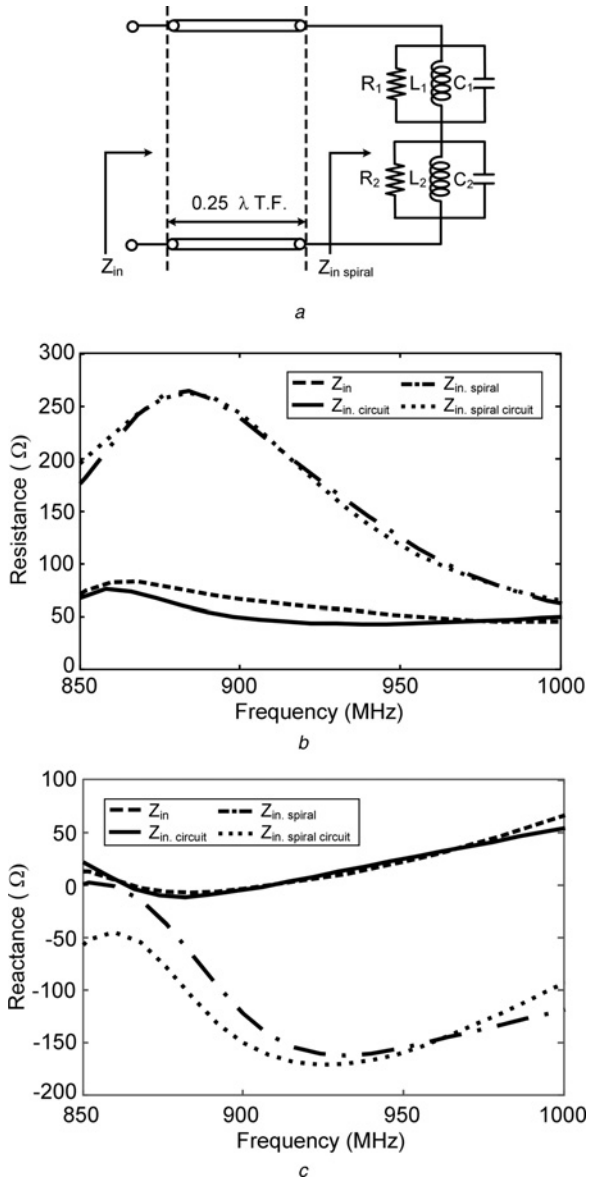

Figure 8 *Impedance by the equivalent circuit model and the EM simulation*

a Equivalent circuit model
b Resistance
c Reactance
Solid and dashed lines represent the input impedance of the total antenna body including the feed line. The dash-dotted and dotted lines represent the input impedance of the double spiral arms excluding the feed line

trial-and-error data fitting by comparing the simulated impedance with the circuit impedance ($R_1 = 240\ \Omega$, $R_2 = 1\ \text{k}\Omega$, $C_1 = 6.3$ pF, $C_2 = 8.9$ pF, $L_1 = 5.1$ nH and $L_2 = 4.3$ nH) [26]. The resistance and reactance obtained using the equivalent circuit model and the simulation are shown in Figs. 8*b* and 8*c*, respectively. The result shows a very high input impedance of about $200 - j100\ \Omega$. These figures clearly show that the feed line works as a quarter-wave transformer that steps down the high impedance of the spiral arm to the $50\ \Omega$ of the coaxial feed over a broad bandwidth.

Fig. 9 shows a comparison of the AR bandwidth for various ground plane sizes, with and without folding the edge of the ground plane. The AR bandwidth covers the full UHF RFID band with an unfolded ground plane more than 18 cm in length. A folded ground plane of only 14 cm gives the same result. The results of this comparison confirm that the folded ground plane is the more effective structure, as it allows a smaller ground plane size without affecting the CP characteristics.

Fig. 10 shows the effect of the number of layers on the antenna performance. As the number of layers increases from 1 to 4, the CP bandwidth (AR < 3 dB) remains nearly unchanged whereas the impedance bandwidth ($S_{11} < -10$ dB) decreases somewhat from 19 to 12%. The minimum volume of the antenna can be achieved with two layers. These results show that the proposed antenna achieves the maximum performance when it has two-layered spiral arms and a fold of 0.06 λ in the ground plane.

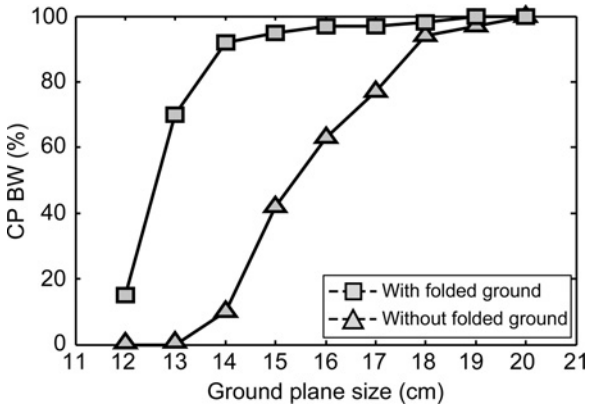

Figure 9 *CP bandwidth as a function of the ground plane size*

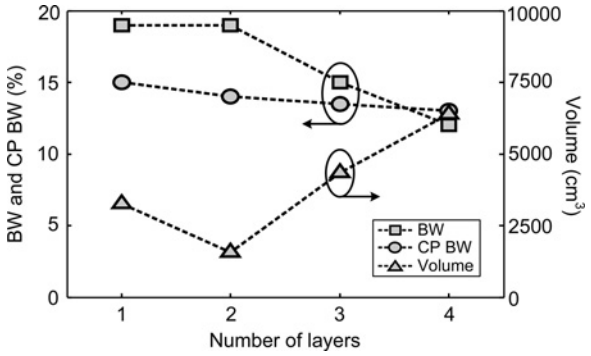

Figure 10 *Impedance bandwidth, CP bandwidth, and volume in terms of the number of layers*

4 Conclusion

In this paper, we described the design of a DLSA with a broad impedance and CP bandwidths for use as a UHF-band RFID reader. The prototype DLSA had an impedance bandwidth of 17% (805–960 MHz) and a CP bandwidth of 20% (850–1000 MHz), which cover the full UHF RFID band (860–960 MHz). The measured gain of the DLSA approached 6.7 dBi. The broad CP operation was due to the induced current on the spiral arm, and the broad impedance bandwidth was explained using an RLC equivalent circuit model. The performance results show that the DLSA would be practical in RFID applications because of its broadband characteristic and small size.

5 Acknowledgment

This work was supported by LS Industrial Systems Co. Ltd.

6 References

[1] KLAUS F.: 'RFID handbook' (Wiley, New York, 2003)

[2] GLIDDEN R., BOCKORICK C., COOPER S., *ET AL.*: 'Design of ultra low-cost UHF RFID tags for supply chain application', *IEEE Commun. Mag*, 2004, **42**, (8), pp. 140–151

[3] HUA R.C., MA T.G.: 'A printed dipole antenna for ultra high frequency (UHF) radio frequency identification (RFID) handheld reader', *IEEE Trans. Antennas Propag*, 2007, **55**, (12), pp. 3742–3745

[4] BOKHARI S.A., ZURCHER J.F., MOSIG J.R., GARDIOL F.E.: 'A small microstrip patch antenna with a convenient tuning option', *IEEE Trans. Antennas Propag*, 1996, **44**, (11), pp. 1521–1528

[5] CHANG N., LIN J.: 'A novel circularly polarized patch antenna with a serial multi-slot type of loading', *IEEE Trans. Antennas Propag*, 2007, **55**, (11), pp. 3345–3348

[6] SONG M., WOO J.: 'Miniaturization of microstrip patch antenna using perturbation of radiating slot', *Electron. Lett.*, 2003, **39**, (5), pp. 417–419

[7] TUNER E.M.: 'Spiral slot antenna' Wright-Patterson AFB, Dayton, OH, Tech. Note WCLR-55-8 WADC, 1995

[8] GARG R., BLARTIA P., BAHL I., ITTIPIBOON A.: 'Microstrip antenna design handbook' (Artech House, Boston, 2001)

doi: 10.1049/iet-map.2008.0315

[9] NAKANO H., OKUZAWA S., OHISHI K., MIMAKI H., YAMAUCHI J.: 'A curl antenna', *IEEE Trans. Antennas Propag.*, 1993, **41**, (11), pp. 1570–1575

[10] MCFADDEN M., SCOTT W.R.: 'Analysis of the equiangular spiral antenna on a dielectric substrate', *IEEE Trans. Antennas Propag.*, 2007, **55**, (11), pp. 3163–3171

[11] NAKANO H., NOGAMI K., ARAI S., MIMAKI H., YAMAUCHI J.: 'A spiral antenna backed by a conducting plane reflector', *IEEE Trans. Antennas Propag.*, 1986, **34**, pp. 791–796

[12] DUTTA ROY S.C.: 'Matching characteristics of the physically short linear impedance transformer', *IEE Proc. Micro. Antennas Propag.*, 2001, **148**, (2), pp. 137–139

[13] COLLIN R.E.: 'Theory and design of wide-band multisection quarter-wave transformers', *IRE Proc.*, 1955, **43**, (2), pp. 179–185

[14] POZAR D.M.: 'Microwave engineering 2/E' (Wiley, New York, 1998), pp. 47–49

[15] KUMAR A., HRISTOV H.D.: 'Microwave cavity antennas' (Artech House, Boston, 1989)

[16] MUSHIAKE Y.: 'An exact step-up impedance ratio chart of folded', *IRE Trans. Antennas Propag*, 1954, **2**, (4), p. 163

[17] CHOO H., LING H.: 'Design of electrically small planar antennas using an inductively coupled feed', *Electron. Lett*, 2003, **39**, (22), pp. 3080–3081

[18] RAHMAT-SAMII Y., MICHIELSSEN E.: 'Electromagnetic optimization by genetic algorithms' (Wiley, New York, 1999)

[19] WEILE D.S., MICHIELSSEN E., GOLDBERG D.E.: 'Genetic algorithm design of Pareto optimal broadband microwave absorbers', *IEEE Trans. Electromagn. Compat.*, 1996, **38**, (3), pp. 518–525

[20] FEKO Software Inc.: FEKO suite 5.3, available at http://www.feko.info/, accessed August 2008

[21] KING R.W.P.: 'Wire and strip conductors over a dielectric-coated conducting or dielectric half-space', *IEEE Trans. Microw. Theory Tech.*, 1989, **37**, (4), pp. 754–760

[22] Regulatory status for using RFID in the UHF spectrum 20 January 2008, available at http://www.epcglobalinc.org/, accessed August 2008

[23] Inpinj Inc.: Speedway, available at http://www.inpinj.com/, accessed August 2008

[24] Alien Technology: ALL 9440, FSA technology, available at http://www.alientechology.com/, accessed August 2008

[25] BALANIS C.A.: 'Antenna theory 3/E: analysis and design' (Wiley, New York, 2005)

[26] EDIMO M., MAHDJOUBI K., SHARAIHA A., TERRET T.: 'Simple circuit model for coax-fed stacked rectangular microstrip patch antenna', *IEE Proc. Microw. Antennas Propag.*, 1998, **145**, (3), pp. 268–272